



## Research Article – Atmosphere Science

# Spatiotemporal observations of CH<sub>4</sub> and CO<sub>2</sub> over Iraq using Atmospheric Infrared Sounder (AIRS) data

Faten G. Abed\*

Ministry of Science and Technology, Space and Communication Directorate, Atmosphere and Space Center, Baghdad, Iraq

(Received: 12-03-2020; Accepted 01-09-2020; Published Online 08-09-2020)

\*Corresponding author (E-mail: Faten\_alzubaidi@yahoo.com)

### Abstract

Methane (CH<sub>4</sub>) and carbon dioxide (CO<sub>2</sub>) are the most important greenhouse gases and most important climate forcing agents due to their significant impact on climate, and their concentrations have been increased since the pre-industrial time by 150 and 40 % respectively, basically from fossil fuel combustion and land-use change emissions. In this research, the atmospheric concentration of CH<sub>4</sub> and CO<sub>2</sub> over Iraq is measured by the Atmospheric Infrared Sounder (AIRS). Time series and time-averaged maps were generated to study and analyse the distribution of CH<sub>4</sub> and CO<sub>2</sub> concentrations. The results show a significant increase of these two gases with an average increase (3.5 and 5.11 ppbv/ year ) in a rate of (2.69 % and 4 %) for CH<sub>4</sub> at SPL 925 hPa and 400 hPa, respectively; the average increase of CO<sub>2</sub> is (1.85 ppm/ year) represent (3.31%) for the whole period. The considerable increase of CH<sub>4</sub> and CO<sub>2</sub> concentration can affect human healthiness and earth radiative balance. Also, the Satellite observation of AIRS can efficiently show the spatiotemporal variations of CH<sub>4</sub> and CO<sub>2</sub> for the study area.

**Key words:** Methane CH<sub>4</sub>-volum mixing ratio, Carbon dioxide CO<sub>2</sub>, AIRS, time series

### Introduction

Methane (CH<sub>4</sub>) and carbon dioxide (CO<sub>2</sub>) are most important climate forcing agent due to their significant impact on climate; CH<sub>4</sub> contributes approximately 17 %, about 0.509 W.m<sup>-2</sup> (Watt/square meter), and CO<sub>2</sub> contributes approximately 66%, about 2.013 W.m<sup>-2</sup>, of the total radiative forcing (RF) by Long-Lived greenhouse gases (LLGHG's), about 3.062 W.m<sup>-2</sup> in 2017. CO<sub>2</sub> is responsible for 82 % of the increased RF over the past ten years particularly the past five years (Butler and Montzka 2018). The atmospheric concentrations of CH<sub>4</sub> and CO<sub>2</sub> have been increased since the pre-industrial time by 150 and 40 % respectively, basically from fossil fuel combustion and land-use change emissions (Sreenivas et al. 2016).

CH<sub>4</sub> is released into the atmosphere by natural and anthropogenic sources. The natural sources such as wetlands and termites contribute 40%, the rest 60 % of the total emission are from the anthropogenic sources mainly from fossil fuel combustion. The atmospheric CH<sub>4</sub> reached 257 % of the pre-industrial level approximately 722 ppb (part per billion) due to the increasing emissions from anthropogenic sources, and then it stabilized until 2006. Since 2007, CH<sub>4</sub> in the atmosphere has increased again. The recent increase in CH<sub>4</sub> emissions is likely from wetlands in the tropics and anthropogenic sources in the mid-latitudes of the northern hemisphere. Whereas in 2017, atmospheric CO<sub>2</sub> reached 146 % of the pre-industrial level-approximately 278 ppm (part per million) reflected the balance among three systems; the atmosphere, the ocean, and the land biosphere (Quééré et al., 2018). Many reasons have contribute the recent CO<sub>2</sub> increase, mostly are from the fossil fuel combustion and cement production emissions, deforestation, and other land-use change as well as due to in part to increased natural emissions of CO<sub>2</sub> connected to the most recent El Nino

event. The mean annual absolute increase of the last 10 years for CH<sub>4</sub> and CO<sub>2</sub> are 6.9 ppb.year<sup>-1</sup> and 2.24 ppm year<sup>-1</sup>, respectively (Butler and Montzka, 2018).

The air mole fractions of CH<sub>4</sub> and CO<sub>2</sub> in the atmosphere have been investigated in many studies using many methods and data sets. Many reasons are submitted of the recent rapid increase; The absence of vegetation cover and the shortage of CO<sub>2</sub> removal process causes an increase in CO<sub>2</sub> concentrations in the atmosphere (Al-Bayati and Al-Salihi, 2019). The determination of the CO<sub>2</sub> growth rates confirmed the record large rates attributed to the 2015-2016 El Nino (Buchwitz et al., 2018). The amplitude of the seasonal variation of CO<sub>2</sub> retrieved from AIRS is related to altitude and coverage (Cao et al., 2019), whilst the seasonal evolution of CO<sub>2</sub> is closely related to the transport of the wind field, removal of precipitation and absorption of vegetation (ChuanBo et al., 2018). Also, the large increase for CO<sub>2</sub> is responding to the global increasing emissions of GHGs and the El Nino effects (Rajab et al., 2014). The ENSO( El Niño-Southern Oscillation ) effect can influence the CO<sub>2</sub> concentration in the mid-troposphere and it's a major source of inter-annual variability in atmospheric CO<sub>2</sub> growth rates (Jiang et al. 2016; Atique, Mahmood, and Atique, 2014) as well as ENSO can affect 36 % of the variability in CH<sub>4</sub> also (Schaefer et al., 2018). The rapid increase of CH<sub>4</sub> in 2014, 2015 and 2017 is consequently either a change in the relative ratios (and totals) of emissions from the biogenic, the thermo-genic and the pyrogenic sources, or a decline in the atmosphere sink of CH<sub>4</sub>, or both (Nisbet et al., 2019). The CH<sub>4</sub> mixing ratio considerable increase is due to the increasing emissions from natural and anthropogenic sources (Abed et al., 2017). And it is largely associated with changing synoptic meteorology (Kavitha et al., 2018). A pronounced variability of CH<sub>4</sub> is in response to

ENSO related precipitation changes (Ribeiro *et al.*, 2016).

As one of the developing countries in Asia, Iraq has fewer emission controls that release a significant amount of CH<sub>4</sub> and CO<sub>2</sub> in the atmosphere. It is one of the top five CH<sub>4</sub> emitters from oil and natural gas systems in the world (EPA, 2013). Besides, Iraq is one of Middle East countries; its economic growth is affected significantly by industrialization, urbanization, and the rapid traffic growth. The intense pollution emissions that produced in major industrial zones, office buildings, manufacturing facilities, a dramatic increase in the number of residences, and increases in the number of motor vehicles (Mossa *et al.*, 2012) all these factors can contribute to the increasing levels of CH<sub>4</sub> and CO<sub>2</sub> in the atmosphere.

This study was originated to study and analyse the spatiotemporal distribution of the average values of CH<sub>4</sub> (2003 – 2016) and CO<sub>2</sub> (2010 -2016) over Iraq by employing the retrieved data of AIRS monthly CH<sub>4</sub> product (AIRX35TM-Ver.6) and monthly CO<sub>2</sub> product (AIRS3CTM-Ver.5). Time series data of CH<sub>4</sub> and CO<sub>2</sub> were analysed also to identify the intensive increase of these two gases through the study period.

### Study Area

Iraq is one of the south-western countries of Asia; located between (38° 45' -48° 45'E) longitude and between (29° 05' -37° 22'N) latitude, see figure 1. From the north; it is bordered by Turkey. Iran is from the east. Jordan, Syria and Saudi Arabia are from the west; Kuwait and Arab gulf are from the south. The total area of Iraq is about 438320 km<sup>2</sup>. Its topography includes four types; the alluvial plain is the first part which occupies a quarter of the total area of Iraq and extends from the north of Baghdad into the south to the Arabian Gulf, this area is flat and embraces 19425 km<sup>2</sup> of marshlands. The second part includes the desert plateau located in the west of alluvial plain and comprises less than half of Iraq's total area; this arid steppe area is extended to Syria, Jordan, and Saudi Arabia. The third part is the mountain region located in the north and northeast of Iraq including the highest altitude reach 3550 meters above sea level. The fourth part is the rolling upland between Tigris and Euphrates rivers; it is a transition area between the alluvial plain in the south and the mountain region in the north and northeast (Abed *et al.*, 2017).

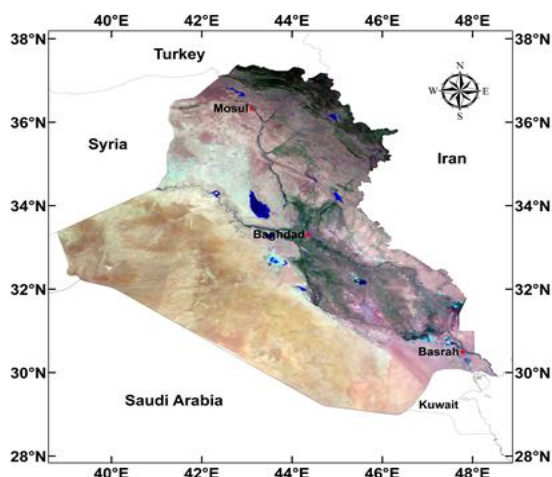


**Figure 1.** The geographical location of the study area (Iraq)

### Data acquisition, specification, and the methodology

Methane volume mixing ratio (CH<sub>4</sub> VMR) and mid-tropospheric carbon dioxide (CO<sub>2</sub>) data are obtained from AIRS - NASA Giovanni online data portal for the study area (Iraq). The infrared thermal sounder (AIRS) is one of the several instruments was launched onboard NASA's EOS AQUA platform on 4 May, 2002 used for earth's weather and climate research, the polar orbit altitude of AIRS reach 705 km with global coverage due to the 1650 km cross-track scanning swath, the equator crossing time is 01:30/13:30 local time and the spatial resolution field of view (FOV) is 13.5 km at nadir. AIRS monitors the complete globe, 95% coverage of earth surface, twice per day by employing 2378 channels at high spectral resolution  $\lambda/\Delta\lambda=1200$  with low noise, the spectral coverage range of AIRS covers from 649-1136, 1217-1613 and 2169-2674 cm<sup>-1</sup> (Abed *et al.*, 2017).

The most important gases retrieved from AIRS are CH<sub>4</sub> and CO<sub>2</sub>. AIRS version 6-L3 provide three products; daily, 8 days and monthly for 28 pressure levels for CH<sub>4</sub> VMR. (VMR; is the ratio of the number density of the gas to the total number density of the atmosphere where density is the number of molecules per unit volume) (Fishbein *et al.*, 2007), each product is provided separate data of daytime (ascending) and night time (descending). The spectral resolution of the monthly CH<sub>4</sub> VMR is averaged and binned into a 1°x1° grid cell. The Grid maps coordinate is ranging from -180.0 ° to +180.0 ° for longitude and from 90.0 ° to +90.0 ° for latitude. Many parameters such as the atmospheric temperature profiles, water vapor profile, surface temperature, and surface emissivity are required as inputs to compute CH<sub>4</sub> retrieval data. CH<sub>4</sub> concentration is measured in part per billion by volume (ppbv) with peak sensitivity at 400 hPa (Olsen *et al.*, 2007).

AIRS also provides retrieval data of monthly mid-tropospheric CO<sub>2</sub> for day and night time under clear and cloudy conditions over ocean and land every day in high spectral resolution and stability, making it ideal for mapping the distribution and transport of CO<sub>2</sub> (Olsen and Licata, 2009). The CO<sub>2</sub> spectral radiance is located in 712-750 cm<sup>-1</sup> region (mid-troposphere at a nadir with spatial resolution 90x90 km<sup>2</sup>) uses an analytical method based on the properties of partial derivatives for the determination of CO<sub>2</sub>. Version 5 -L3 carbon dioxide data have averaged and binned into (2° latitude x 2.5° longitude) grid map (dimensions of those files are 91° latitude x 144° longitude). The CO<sub>2</sub> concentration is measured in part per million (ppm) this is the mole fraction of CO<sub>2</sub>, It is the total tropospheric column feature. The retrievals of AIRS are based on cloud-cleared thermal infrared radiance spectra in the 15-micron band and related Level 2 geophysical profiles of temperature, water vapor, and ozone, and achieve 2 ppm accuracy in the tropics and mid-latitudes (Zhang *et al.*, 2014; Rajab *et al.*, 2014).

The monthly averaged maps of CH<sub>4</sub> and CO<sub>2</sub> were generated using the IDW (Inverse Distance Weighted) interpolation technique which can be defined as a tool that uses an interpolation method to estimate cell values by calculating the mean values of sample data points in the neighborhood for each processing cell. The closer the point to the center of the cell being assessed, the greater the effect or weight it has in the centering process. This technique was applied on the 2D raster data of CH<sub>4</sub> and CO<sub>2</sub> that converted

in to point vector format to interpolate the concentration for assessing the spatial distribution. The CH<sub>4</sub> and CO<sub>2</sub> concentrations were specified by using the area average over the entire study area for graphical analysis. The time-series of the monthly average data of CH<sub>4</sub> and CO<sub>2</sub> were plotted using Sigma-plot software.

**Results and Discussion**

Time series and time-averaged maps were analyzed to observe the spatiotemporal variations in the concentration of CH<sub>4</sub> and CO<sub>2</sub>. The observed variation can be attributed to anthropogenic activities based on the spatial extent of each gas. CH<sub>4</sub> VMR data for SPL- 925 and 400 hPa was utilized from January 2003 to September 2016 for Iraq. The standard pressure level SPL at 925 hPa is the second closest level to earth surface while the pressure level at 400 hPa is the most sensitive level by AIRS CH<sub>4</sub> retrieval. A significant increase in CH<sub>4</sub> concentration was observed from 2003 to 2016, the CH<sub>4</sub> average concentration of 925 hPa in 2003 was (1823.96 ppbv) which is increased up to (1873.09 ppbv) in 2016 lead to an average increase of (3.5 ppbv/year) and the CH<sub>4</sub> average concentration of 400 hPa in 2003 was (1791.47 ppbv) which is increased up to (1863.13 ppbv) in 2016 lead to an average increase of (5.11 ppbv/year), this indicates an average CH<sub>4</sub> value of (1844.56 ± 17.83 ppbv) and (1824.09 ± 33.99 ppbv) for the whole study period with significant increase of (2.69 %) and (4 %) for both SPL- 925 and 400 hPa respectively (Figure 2 a-b)

For CO<sub>2</sub>, a significant increase is observed from January 2010 to December 2016, the CO<sub>2</sub> average concentration was (390.37 ppm) in 2010 which increased up to (403.32 ppm) in 2016 leading to an increase of (1.85ppm/year). This indicates an average CO<sub>2</sub> value of (396.69 ± 4.57 ppm) for the whole study period with a significant increase of (3.31%). In one hand, the steady increase in CH<sub>4</sub> and CO<sub>2</sub> concentrations can be attributed to the global increase due to increasing emissions from its natural and anthropogenic sources accompanied with a decrease in removal process in the other hand, besides the transport effect which redistribute the pollutants through convection and advection due to the large scale dynamics of earth's atmosphere (Le Quéré *et al.*, 2009), see Figure 2- c.

Time-averaged map of CH<sub>4</sub> VMR distribution at SPL- 925 and 400 hPa during the study period shows a large values of CH<sub>4</sub> in the area located in the north and north-east parts of Iraq, see figure 3- a and b, might be related to the meteorology which cap the pollutants at these heights, as well as the diverse sources of CH<sub>4</sub> encompass the natural and anthropogenic. the northern area has nine months of growing season in a year and the cultivated area by rain-fed crop fields of rice is emit large amount of CH<sub>4</sub> as a result of the anaerobic decomposition process of organic material by methanotrophic bacteria in a flooded soil and sediment (Lagzi *et al.*, 2014; Smith *et al.*, 2010) , besides northern area of Iraq has an average annual rainfall over 400 to1000 mm thus the pastureland is in a good condition leading to increase the livestock population hence more CH<sub>4</sub> emission. The anthropogenic emission due to the human activities and the industry also contribute the increasing levels of CH<sub>4</sub>. Moreover, Winds can carry pollutants from their sources due to the transport effect which affected by the atmospheric conditions such as temperature, pressure, and humidity besides the local weather patterns. The less concentrations of

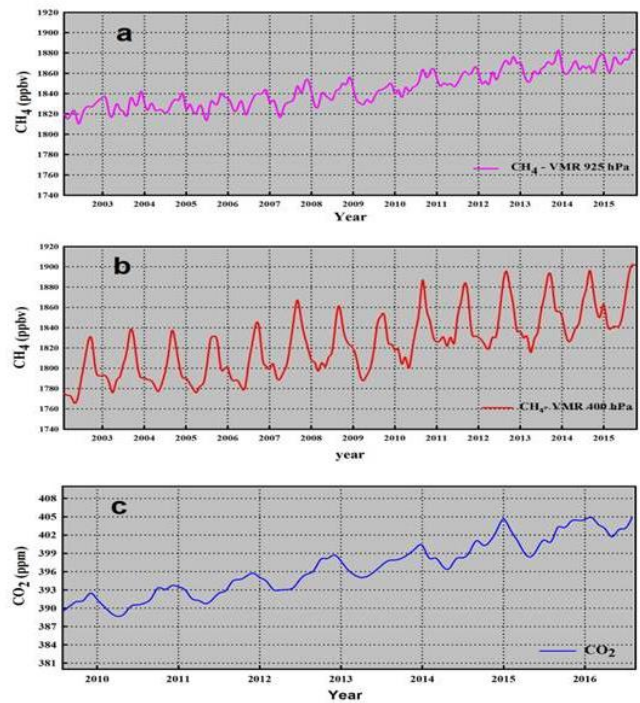


**Figure 2: a and b** shows the long-term time series of CH<sub>4</sub> at 925 hPa and 400 hPa between 2003 and 2016 and 2-C. for CO<sub>2</sub> between 2010 and 2016 of the study area (Iraq)

CH<sub>4</sub> VMR are appeared in the western- south part of Iraq due to several reasons; firstly it is a barren area that can acts as a sink for CH<sub>4</sub> due to the dry soil oxidation (Zhang *et al.*, 2014). Secondly, it is sparsely populated and cultivated with a just few crops in some irrigation spots which means a lack of CH<sub>4</sub> sources (Abed *et al.*, 2017). Most of the central areas of Iraq have a moderate range of CH<sub>4</sub> concentrations.

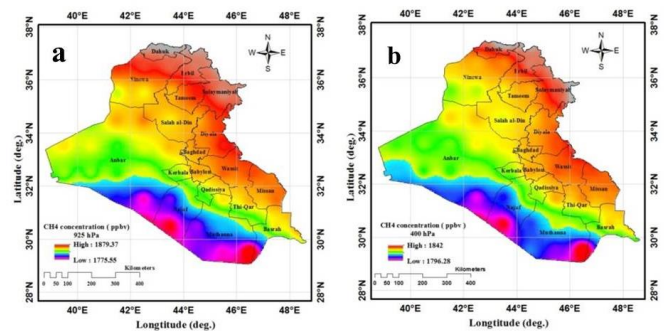


**Figure 3 - a, b.** Shows the spatiotemporal distribution of the averaged CH<sub>4</sub> VMR concentration over Iraq for SPL (925 and 400 hPa) for the period between 2003 and 2016.

The Spatial distribution of CO<sub>2</sub> is in contrast with CH<sub>4</sub> during the study period over Iraq. The highest concentration of CO<sub>2</sub> has appeared over the western and southern parts of Iraq. The desert covers most parts of the western area of Iraq and the arid climate has dominated these regions where no vegetation grows thus the removal process of CO<sub>2</sub> is weakened due to the limits of CO<sub>2</sub> fertilization on land and the decrease in carbonate concentrations cause the lack of CO<sub>2</sub> removal process. The southern part of Iraq also has a high concentration of CO<sub>2</sub> due to the abundance of oil and gas fields as well as it is densely populated region and human activities increase's the CO<sub>2</sub> emissions particularly from the fossil fuel composition beside the presence of cement production factories. The moderate and less concentration is

appeared in most parts of Iraq including the alluvial plain area due to vegetation growth which is considered as a large natural sink of CO<sub>2</sub> that consumes CO<sub>2</sub> via the photosynthesis process (Le Quéré *et al.*, 2009), see figure 4. The main processes that remove CO<sub>2</sub> primarily at the surface include biological (photosynthesis) and physical (solubility) (Buchwitz *et al.*, 2018).

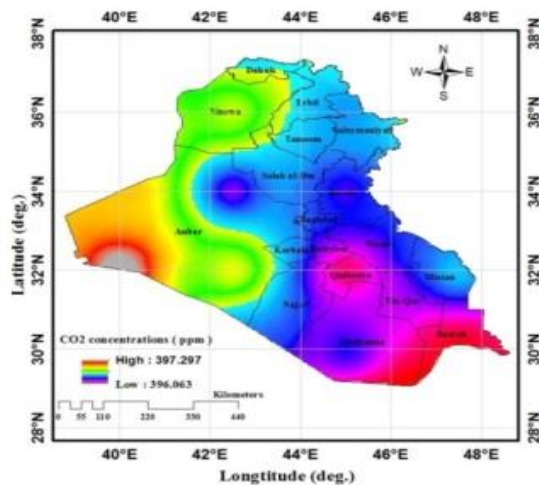


**Figure 4.** Show the spatiotemporal distribution of the averaged CO<sub>2</sub> concentration over Iraq for the period between 2010 and 2016.

## Conclusions

A significant increase in CH<sub>4</sub> and CO<sub>2</sub> concentrations were observed through study period with an average increase of 3.5 and 5.11 ppbv/ year for CH<sub>4</sub> at 925 and 400 hPa, respectively. an increase of 1.85 ppm/year for CO<sub>2</sub>; this steady increase of CH<sub>4</sub> and CO<sub>2</sub> can be attributed to the global increase due to increasing emissions from the natural and anthropogenic sources accompanied with a decrease in removal process. The time average maps illustrate large values of CH<sub>4</sub> for both 925 and 400 hPa over the area located in the north and north-east parts of Iraq mostly due to increasing emissions from the natural sources, While the less concentrations have appeared in the western south part of Iraq, and the central area of Iraq has moderate values through the whole study period. In contrast, the CO<sub>2</sub> large concentrations appeared over the western area because of the arid climate is dominates these regions where no vegetation grows. The southern parts of Iraq also have large values of CO<sub>2</sub> due to fossil fuel composition from oil and gas fields; the moderate and less value have appeared in most parts of Iraq including the alluvial plain area. The substantial increase in this concentration can affect human health and earth radiative balance.

## References

- Abed, F.G., Al-Salihi, A.M., and Rajab, J.M. (2017). Spaceborne observation of methane from atmospheric infrared sounder: data analysis and distribution over Iraq. *Journal of Applied and Advanced Research*, 4, 256-64.
- Al-Bayati, R.M., and Al-Salihi, A.M. (2019). Monitoring carbon dioxide from (AIRS) over Iraq during 2003-2016. In *AIP Conference Proceedings*, 030007. AIP Publishing.
- Atique, L., Mahmood, M., and Atique, F. (2014). Disturbances in atmospheric radiative balance due to anthropogenic activities and its implications for climate change. *American-Eurasian Journal of Agricultural and Environmental Sciences*, 14 (1), 73-84.
- Buchwitz, M., Reuter, M., Schneising, O., Noël, S., Gier, B., Bovensmann, H., Burrows, J. P., Boesch, H., Anand, J., Parker, R. J., Somkuti, P., Detmers, R. G., Hasekamp, O. P., Aben, I., Butz, A., Kuze, A., Suto, H., Yoshida, Y., Crisp, D., and O'Dell, C. (2018). Computation and analysis of atmospheric carbon dioxide annual mean growth rates from satellite observations during 2003–2016. *Atmospheric Chemistry and Physics*, 18, 17355–17370.
- Butler, J.H., and Montzka, S.A. (2018). The NOAA annual greenhouse gas index (AGGI), <http://www.esrl.noaa.gov/gmd/aggi/aggi.html>.
- Cao, L., Chen, X., Zhang, C., Kurban, A., Qian, J., Pan, T., Yin, Z., Qin, X., Ochege, F.U., Maeyer, P.D. (2019). The Global Spatiotemporal Distribution of the Mid-Tropospheric CO<sub>2</sub> Concentration and Analysis of the Controlling Factors. *Remote Sensing*, 11, 94.
- ChuanBo, F., Li, D., Ming, F.J., Jing, P., and Na, Y. (2018). Temporal and spatial heterogeneous distribution of tropospheric CO<sub>2</sub> over China and its possible genesis. *Journal of Geophysics-Chinese Edition*, 61, 4373-82.
- EPA, US. 2013. Global mitigation of non-CO<sub>2</sub> greenhouse gases: 2010-2030. In: United States Environmental Protection Agency Washington (DC).
- Fishbein, E., Granger, S., Lee, S.Y., Manning, E., Weiler, M., Blaisdell, J., and Susskind, J. (2007). 'AIRS/AMSU/HSB Version 5 Data Release User Guide, Atmospheric Infrared Sounder, A., EOS.'
- Jiang, X., Crisp, D., Olsen, E. T., Kulawik, S. S., Miller, C. E., Pagano, T. S., Liang, M., and Yung, Y. L. (2016). CO<sub>2</sub> annual and semiannual cycles from multiple satellite retrievals and models. *Earth and Space Science*, 3, 78-87.
- Kavitha, M., Nair, P.R., Girach, I.A., Aneesh, S., Sijikumar, S., and Renju, R. (2018). Diurnal and seasonal variations in surface methane at a tropical coastal station: Role of mesoscale meteorology. *Science of the Total Environment*, 631, 1472-1485.
- Lagzi, I., Meszaros, R., Gelybo, G., and Leelossy, A., (2014). Atmospheric chemistry, Eotvos Lorand University.
- Le Quéré, C., Raupach, M.R., Canadell, J.G., Marland, G., Bopp, L., Ciais, P., Conway, T.J., Doney, S.C., Feely, R.J., and Foster, P. (2009). Trends in the sources and sinks of carbon dioxide. *Nature Geoscience*, 2, 831.
- Nisbet, E. G., Manning, M. R., Dlugokencky, E. J., Fisher, R. E., Lowry, D., Michel, S. E., Myhre, C.L., Platt, S. M., Allen, G., and Bousquet, P. (2019). Very strong atmospheric methane growth in the 4 years 2014–2017: Implications for the Paris Agreement. *Global Biogeochemical Cycles*, 33, 318-42.
- Olsen, E. T., and Licata, S. J. (2009). AIRS version 5 release tropospheric CO<sub>2</sub> products. In: Jet Propulsion Laboratory, California Institute of Technology, Pasadena, California.

- Olsen, E.T., Elliott, D., Fetzer, E., Fishbein, E., Granger, S., Lee, S.Y., Manning, E., Blaisdell, J., and Susskind, J. (2007). AIRS/AMSU/HSB version 5 data disclaimer. In: *Atmospheric Infrared Sounder, A., EOS.* Goddard Space Flight Center, NASA, Jet Propulsion Laboratory, California Institute of Technology, Pasadena, CA
- Quééré, C., Andrew, R. M., Friedlingstein, P., Sitch, S., Pongratz, J., Manning, A. C., Korsbakken, J. I., Peters, G. P., Canadell, J. G., and Jackson, R. B., (2018). Global carbon budget 2017. *Earth System Science Data*, 10, 405-448.
- Rajab, J. R., Ahmed, H. S., and Mossa, H. A. (2012). Analysis of Troposphere Carbon Dioxide in IRAQ from Atmosphere Infrared Sounder (AIRS) data: 2010-2011. *Journal of University of Babylon*, 22(1), 524-531.
- Rajab, J., Lim, H-S., and Jafri, M. M. (2014). Investigation on the interannual variability of Troposphere Carbon Dioxide from (AIRS) in Peninsular Malaysia: 2003-2009. In *International Conference on Natural and Environmental Science (ICONES)*, 29-35.
- Ribeiro, I.O., Rodrigo de Souza, A. F., Andreoli, R. V., Kayano, M. T., and Costa, P. S. (2016). 'Spatiotemporal variability of methane over the Amazon from satellite observations. *Advances in Atmospheric Sciences*, 33, 852-864.
- Schaefer, H., Smale, D., Nichol, S. E., Bromley, T. M., Brailsford, G. W., Martin, R. J., Moss, R., Michel, S. E., and White, J. W. C. (2018). Limited impact of El Niño–Southern Oscillation on variability and growth rate of atmospheric methane, *Biogeosciences*, 15, 6371-6386.
- Smith, P., Reay, D., and Amstel, A. V. (2010). *Methane and climate change* (Earthscan Ltd, UK, Earthscan LLC, USA: UK).
- Sreenivas, G., Mahesh, P., Subin, J., Kanchana, A. L., Rao, P. V. N., and Dadhwal, V. K. (2016). Influence of meteorology and interrelationship with greenhouse gases (CO<sub>2</sub> and CH<sub>4</sub>) at a suburban site of India. *Atmospheric Chemistry and Physics*, 16, 3953-3967.
- Zhang, Y., Xiong, X., Tao, J., Yu, C., Zou, M., Su, L., and Chen, L. (2014). Methane retrieval from Atmospheric Infrared Sounder using EOF-based regression algorithm and its validation. *Chinese Science Bulletin*, 59, 1508-1518.